Nucleus 3:5, 452-462; September/October 2012; © 2012 Landes Bioscience

Blocking farnesylation of the prelamin A variant in Hutchinson-Gilford progeria syndrome alters the distribution of A-type lamins

Yuexia Wang,[1,2] Cecilia Östlund,[1,2] Jason C. Choi,[1,2] Theresa C. Swayne,[3] Gregg G. Gundersen[2] and Howard J. Worman[1,2,*]

[1]Department of Medicine; College of Physicians and Surgeons; Columbia University; New York, NY USA; [2]Department of Pathology and Cell Biology; College of Physicians and Surgeons; Columbia University; New York, NY USA; [3]Herbert Irving Comprehensive Cancer Center; College of Physicians and Surgeons; Columbia University; New York, NY USA

Keywords: lamin, nuclear envelope, progeria, farnesylation, inner nuclear membrane, progerin

Abbreviations: AVI, Audio Video Interleave; FRET, fluorescence resonance energy transfer; FTI, protein farnesyltransferase inhibitor; FRAP, fluorescence recovery after photobleaching; GFP, green fluorescent protein; GFP-progerin-NF, GFP-non-farnesylated progerin; HGPS, Hutchison-Gilford progeria syndrome; LAP1, lamina-associated polypeptide 1; MEFs, mouse embryonic fibroblasts; PCNA, proliferating cell nuclear antigen; RFP, red fluorescent protein; RNAPII, DNA-dependent RNA polymerase II

Mutations in the lamin A/C gene that cause Hutchinson-Gilford progeria syndrome lead to expression of a truncated, permanently farnesylated prelamin A variant called progerin. Blocking farnesylation leads to an improvement in the abnormal nuclear morphology observed in cells expressing progerin, which is associated with a re-localization of the variant protein from the nuclear envelope to the nuclear interior. We now show that a progerin construct that cannot be farnesylated is localized primarily in intranuclear foci and that its diffusional mobility is significantly greater than that of farnesylated progerin localized predominantly at the nuclear envelope. Expression of non-farnesylated progerin in transfected cells leads to a redistribution of lamin A and lamin C away from the nuclear envelope into intranuclear foci but does not significantly affect the localization of endogenous lamin B1 at nuclear envelope. There is a similar redistribution of lamin A and lamin C into intranuclear foci in transfected cells expressing progerin in which protein farnesylation is blocked by treatment with a protein farnesyltransferase inhibitor. Blocking farnesylation of progerin can lead to a redistribution of normal A-type lamins away from the inner nuclear envelope. This may have implications for using drugs that block protein prenylation to treat children with Hutchinson-Gilford progeria syndrome. These findings also provide additional evidence that A-type and B-type lamins can form separate microdomains within the nucleus.

Introduction

Hutchinson-Gilford progeria syndrome (HGPS; OMIM no. 176670) is a rare, sporadic, dominant genetic disorder characterized by phenotypic features of accelerated aging.[1,2] It is caused by de novo mutations in *LMNA*, the gene encoding A-type nuclear lamins.[3,4] Lamins are intermediate filament proteins that polymerize to form the nuclear lamina, which is located on the inner aspect of the inner nuclear membrane of nucleated metazoan cells.[5-8] The major A-type lamins expressed in somatic cells, lamin A and lamin C, arise by alternative RNA splicing. They are identical for their first 566 amino acids and differ in their carboxyl-termini, with lamin C having six unique amino acids encoded by *LMNA* exon 10 and prelamin A, the precursor to lamin A, having 98 unique amino acids encoded by exons 11 and 12.[9] Mutations causing HGPS (G608G or G608S) create an abnormal splice donor site within RNA encoded by exon 11, leading to an in-frame deletion of 50 amino acids from prelamin A.[3,4] This truncated prelamin A variant expressed in HGPS has been named progerin.

Prelamin A contains a cysteine-aliphatic-aliphatic-any amino acid (CAAX) motif of sequence cysteine-serine-isoleucine-methionine (CSIM) at its carboxyl-terminus. This motif initiates a series of enzymatic reactions leading to farnesylation of the cysteine, cleavage of -SIM and carboxymethylation of the cysteine.[10,11] Farnesylated prelamin A is then recognized by the endoprotease ZMPSTE24 and cleaved 15 amino acids from the farnesylated carboxyl-terminal cysteine to yield lamin A.[11,12] As a consequence of the 50 amino acid deletion, progerin does not contain this ZMPSTE24 cleavage site. Progerin therefore retains a farnesyl-cysteine methyl ester at its carboxyl-terminus.

Progerin is believed to exert its effects on cells via a dominant, toxic mechanism.[13] An obvious effect of progerin expression in cells is a significant change in nuclear shape, including abnormalities visualized at the light microscopy level such as lobulations or "blebs" in the nuclear envelope, "folds" in the nuclear envelope,

*Correspondence to: Howard J. Worman; Email: hjw14@columbia.edu
Submitted: 05/17/12; Revised: 07/28/12; Accepted: 07/31/12
http://dx.doi.org/10.4161/nucl.21675

©2012 Landes Bioscience. Do not distribute

a thickening of the nuclear lamina, loss of peripheral heterochromatin and clustering of nuclear pores.[14] Abnormal nuclear morphology occurs when progerin is expressed at "endogenous pathological" levels, such as in cells from human subjects with HGPS and mice with a "knock in" mutation in the endogenous *Lmna* gene, as well as in cells in which the progerin is expressed by transgenic methods.[3,4,14-31] This prominent morphological abnormality appears to be caused by expression of farnesylated progerin at the nuclear envelope, as blocking protein prenylation significantly restores normal nuclear shape.[16-21,25-27,30] The normalization of nuclear shape induced by blocking progerin prenylation correlates with an amelioration of disease phenotypes in mouse models of HGPS.[32-37]

In cultured cells, normalization of nuclear shape generated by blocking progerin farnesylation leads to the redistribution of the non-prenylated progerin away from the nuclear envelope to the nuclear interior.[16,18-21,27] Expression of progerin with the CSIM sequence signaling farnesylation mutated to SSIM or CSM similarly leads to concentration of progerin away from the nuclear rim in intranuclear foci or other abnormal structures.[18,19,34,37] These observations led to the hypothesis that targeting progerin away from the nuclear envelope/inner nuclear membrane into the nuclear interior by blocking its farnesylation may be responsible for beneficial effects in HGPS.[38] However, the composition and features of the intranuclear foci of non-farnesylated progerin have not been described. And while the dynamics of farnesylated progerin at the nuclear envelope have been examined,[39] the dynamics of non-farnesylated progerin in the nucleoplasm have not been studied. Here we examine the effects of farnesylation on the localization and dynamics of progerin, characterizing the intranuclear foci formed by the non-farnesylated protein and obtaining insights into nuclear lamina formation.

Results

Effects of farnesylation on progerin localization and dynamics. We first set out to confirm that preventing the farnesylation of progerin leads to its redistribution from the nuclear envelope to the inside of the nucleus, as has been observed in other studies.[16,18-21,27] In transiently transfected mouse embryonic fibroblasts (MEFs) analyzed by confocal microscopy, a construct of green fluorescent protein (GFP) fused to the N-terminus of progerin (GFP-progerin) was localized almost exclusively at the nuclear periphery, whereas a GFP-progerin variant that could not be farnesylated because the cysteine of the CAAX motif was changed to a serine (GFP-progerin-NF), was localized primarily in intranuclear foci (**Fig. 1A**; see also **Vid. S1**). In over 50 transfected cells examined, GFP-progerin-NF was localized predominantly in intranuclear foci in approximately 90% of transfected cells and primarily at the nuclear periphery in only 10%. The cells expressing GFP-progerin had irregularly shaped nuclei with blebbing of the nuclear envelope whereas those expressing GFP-progerin-NF were more regular in shape. We then used fluorescence recovery after photobleaching (FRAP) to determine if farnesylation affected the dynamics of progerin. We photobleached a part of nuclear rim of cells expressing GFP-progerin or an internal focus near the edge of the nucleus in cells expressing GFP-progerin-NF for the FRAP experiment. FRAP analysis showed that non-farnesylated progerin in intranuclear foci had a significantly increased diffusional mobility compared with farnesylated progerin localized to the nuclear periphery (**Fig. 1B**). These results confirmed that non-farnesylated progerin is primarily localized in intranuclear foci rather than the nuclear envelope and that it can diffuse more readily within nuclei than the farnesylated protein. To determine if the intranuclear foci of non-farnesylated progerin co-localized with selected nuclear proteins, we performed immunofluorescence analysis of MEFs transiently expressing GFP-progerin-NF with antibodies against PML, proliferating cell nuclear antigen (PCNA), DNA-dependent RNA polymerase II (RNAPII) and heterochromatin protein 1. There was absolutely no co-localization with heterochromatin protein 1 (data not shown) and only partial overlap with PML bodies and the more diffusely localized RNAPII and PCNA (**Fig. 1C**), indicating that intranuclear foci of non-farnesylated progerin did not precisely co-localize with these other nuclear proteins.

Expression of non-farnesylated progerin alters the nuclear distribution of A-type lamins but not lamin B1. We next asked whether the expression of non-farnesylated progerin in intranuclear foci would alter the normal distribution of endogenous A-type lamins. In transiently transfected MEFs examined by confocal microscopy, immunostaining with antibodies against lamin A (which would also recognize progerin fusion proteins but do not recognize lamin C) showed that lamin A and GFP-progerin were co-localized almost exclusively at the nuclear periphery. However, virtually all of the lamin A labeling co-localized with the green fluorescent signal of foci without any smooth nuclear rim labeling in almost all of the cells expressing GFP-progerin-NF (**Fig. 2**; see also **Vid. S2**). This suggested that lamin A has a higher avidity for overexpressed non-farnesylated progerin than for endogenously expressed lamins, leading to a change in its distribution, normally mostly at the nuclear periphery, into discrete foci in the nuclear interior.

We also analyzed the effects of expressing GFP-progerin on the nuclear distribution of the other major A-type lamin, lamin C. Because of the lack of high quality antibodies that specifically recognize lamin C and to clearly distinguish the localization of A-type lamins from that of the progerin fusion proteins, we co-transfected MEFs with plasmids that express either GFP-progerin or GFP-progerin-NF and plasmids that express lamin C with red fluorescent protein (RFP) fused to its N-terminus (RFP-lamin C). In these cells, RFP-lamin C co-localized with GFP-progerin at the nuclear periphery but almost exclusively in intranuclear foci with GFP-progerin-NF (**Fig. 3**; see also **Vid. S3**). Hence, like endogenous lamin A, RFP-lamin C preferentially co-localized with intranuclear non-farnesylated progerin rather than with endogenous lamins at the nuclear envelope.

In contrast to its effect on altering the distribution of A-type lamins from the nuclear envelope to the intranuclear foci, expression of non-farnesylated progerin did not significantly affect the localization of endogenous lamin B1. In transiently transfected MEFs expressing GFP-progerin or GFP-progerin-NF, immunofluorescence labeling showed that endogenous lamin B1 was

©2012 Landes Bioscience. Do not distribute

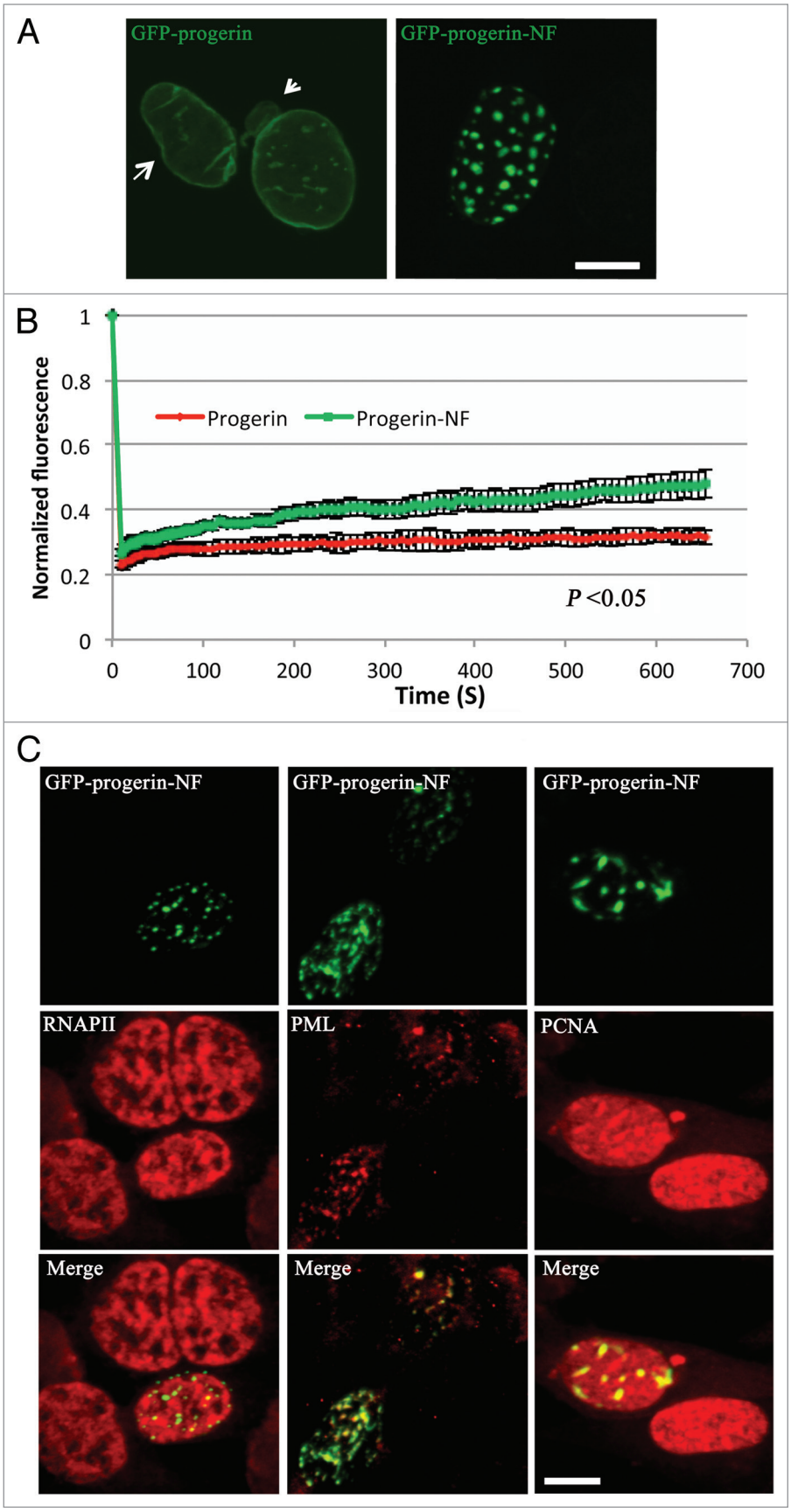

Figure 1. Intracellular localizations and dynamics of progerin and non-farnesylated progerin in transiently transfected MEFs. (A) Confocal fluorescence micrographs showing localizations of GFP-progerin at the nuclear envelope and GFP-progerin-NF in intranuclear foci. The arrow indicates the irregular shape, and the arrowhead points a nuclear envelope bleb in the cells expressing GFP-progerin. Bar: 5 μm. (B) The diffusional mobility of GFP-progerin-NF is higher than that of GFP-progerin in transfected MEFs. Quantitative experiments showing normalized fluorescence recovery after photobleaching in cells transiently transfected with cDNA constructs encoding GFP-progerin (red) or GFP-progerin-NF (green). Normalized fluorescence of 1 is the level before bleaching. Normalized fluorescence for GFP-progerin-NF is statistically significantly higher than that for GFP-progerin ($p < 0.05$ at 13 sec, 22 sec, 31 sec, 61 sec, 102 sec, 302 sec and 654 sec these time points; n = 12 cells analyzed for GFP-progerin and n = 10 cells analyzed for GFP-progerin-NF). Values shown are means plus or minus standard deviations. (C) Confocal immunofluorescence micrographs of transiently transfected MEFs expressing GFP-progerin-NF (green) and labeled with antibodies against RNAPII, PML or PCNA (red) with signal overlap appearing yellow (merge). Bar: 5 μm.

always localized primarily at the nuclear periphery with minimal to no co-localization with GFP-progerin-NF in intranuclear foci (**Fig. 4**; see also **Vid. S4**). Hence, lamin B1 appears to have a higher avidity for the nuclear envelope than for overexpressed intranuclear non-farnesylated progerin.

Effects of treatment with a protein farnesyltransferase inhibitor (FTI) on progerin localization and lamin distribution. To determine how pharmacological blockade of progerin prenylation affects its localization and the distribution of lamins, we treated transfected MEFs with an FTI (FTI-276) for 48 h. Incubation of MEFs with 10 μM of FTI-276 blocked protein prenylation as shown by accumulation of prelamin A, which was approximately equal in amount to lamin A, and non-farnesylated HDJ-2, a permanently farnesylated protein (**Fig. 5A**). In the FTI-treated cells, GFP-progerin was localized primarily in intranuclear foci along with endogenous lamin A/prelamin A (the antibody used recognized both) and RFP-lamin C, whereas lamin B1, which is also a farnesylated protein, remained primarily at the nuclear periphery in almost all of the transfected cells (**Fig. 5B**; see also **Vid. S5**).

©2012 Landes Bioscience. Do not distribute

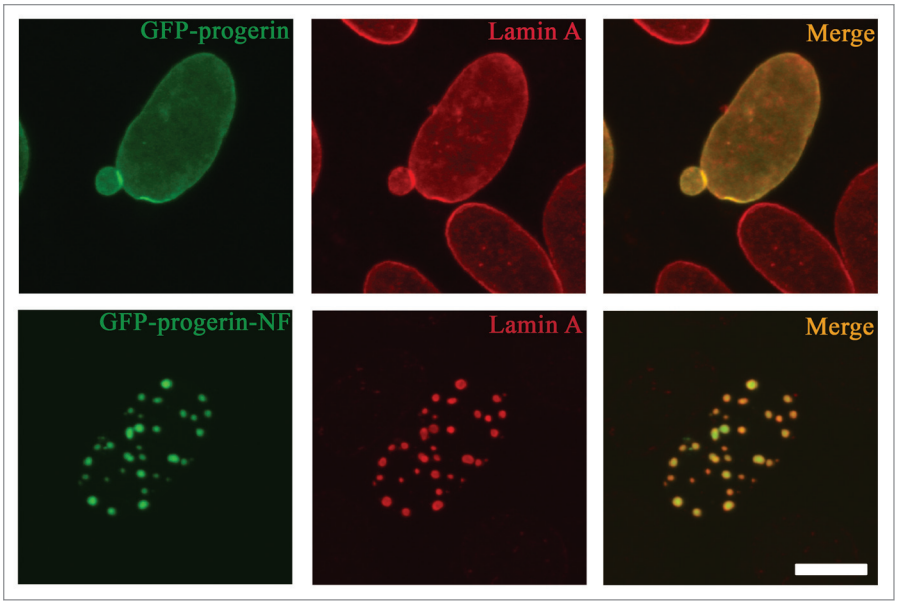

Figure 2. Expression of non-farnesylated progerin alters the nuclear distribution of lamin A in transiently transfected MEFs. Confocal fluorescence micrographs showing localizations of GFP-progerin and GFP-progerin-NF (green signals) and immunofluorescence labeling with anti-lamin A antibodies (red signals) in the same cells; merged images are shown at the right with signal overlap appearing yellow (merge). Bar: 5 μm.

Pharmacological blockade of protein farnesylation used in present experiments therefore had similar effects on the distribution of lamins as did expression of GFP-progerin-NF.

Localizations of integral inner nuclear membrane proteins and nuclear pore complexes in cells expressing progerin or non-farnesylated progerin. We next examined the effects of expressing non-farnesylated progerin on the localizations of two integral proteins of the inner nuclear membrane and nuclear pore complex proteins. We used confocal microscopy to image transiently transfected MEFs expressing GFP-progerin or GFP-progerin-NF and immunostained with antibodies that recognize either lamina-associated polypeptide 1 (LAP1) or emerin, integral proteins concentrated in the inner nuclear membrane, or antibodies that recognize several proteins of the nuclear pore complex. In MEFs expressing GFP-progerin or GFP-progerin-NF, endogenous LAP1 was always localized at nuclear periphery (**Fig. 6A**; see also **Vid. S6**). Endogenous emerin was co-localized with GFP-progerin at nuclear periphery. However, in cells expressing GFP-protein-NF, emerin was localized at both the nuclear periphery as well as in the intranuclear foci with the non-farnesylated progerin variant (**Fig. 6B**; see also **Vid. S6**). Nuclear pore complex localization was not significantly affected by the presence of intranuclear foci of GFP-progerin-NF (**Fig. 6C**).

Interactions of lamin A and lamin C with progerin-NF. As A-type lamins co-localized with non-farnesylated progerin in intranuclear foci, we performed biochemical and biophysical experiments to examine their interactions. First, protein extracts from transiently transfected MEFs expressing GFP-lamin A, GFP-progerin, GFP-progerin-NF or GFP were subjected to co-immunoprecipitation using an anti-GFP antibody and precipitated products detected by immunoblotting with anti-lamin A/C antibodies. Endogenous lamin A and lamin C co-immunoprecipitated with GFP-lamin A, GFP-progerin and GFP-progerin-NF but not GFP; more endogenous A-type lamins appeared to co-immunoprecipitate with GFP-tagged lamin A and non-farnesylated progerin compared with progerin with similar protein inputs into the experiments (**Fig. 7A**). We next used acceptor photobleaching FRET to examine the molecular interactions of lamin A and lamin C with progerin and non-farnesylated progerin in intact cells. In this method, FRET efficiency was measured as an increase in donor fluorescence after acceptor photobleaching. MEFs were co-transfected with plasmids encoding RFP-lamin A, RFP-lamin C or RFP control (acceptors) and GFP-progerin or GFP-progerin-NF (donors). MEFs were also transfected with RFP-lamin A or GFP-progerin only to calculate the cross-talk correction factor and donor bleaching correction factor. An increase in donor fluorescence was detected in nuclei expressing GFP-progerin or GFP-progerin-NF after acceptor photobleaching (**Fig. 7B**). Statistical analysis showed that the energy transfer between GFP-progerin-NF and RFP-lamin A or RFP-lamin C was statistically significantly higher than the transfer between GFP-progerin and RFP-lamin A or RFP-lamin C (**Fig. 7C**), indicating a closer association of wild type A-type lamins with progerin-NF than with progerin. There was no significant energy transfer between GFP-progerin or GFP-progerin-NF and RFP (**Fig. 7C**). Energy transfer was independent of the intensity of acceptor fluorescence (RFP) or donor fluorescence (GFP) in the experiment presented, indicating the FRET was not a random distribution effect (**Fig. 7D**).

Discussion

The fact that blocking farnesylation of prelamin A leads to an intranuclear accumulation of the protein away from the nuclear envelope was first suggested by results obtained by McKeon and colleagues, who showed this for a CAAX motif mutant.[40] Sinensky and colleagues subsequently showed that blocking prelamin A prenylation with lovastatin leads to its intranuclear accumulation.[41] With regards to progerin, Yang et al. first demonstrated in fibroblasts from a gene-targeted mouse model expressing progerin, but not wild type prelamin A, that FTI treatment mis-localized progerin away from the nuclear envelope to the nucleoplasm in discrete intranuclear foci.[16] Several subsequent studies in cultured fibroblasts from human subjects with HGPS or in progerin-transfected cells collectively showed that blocking farnesylation of progerin led to its redistribution away from the nuclear envelope into the nuclear interior, sometimes in

©2012 Landes Bioscience. Do not distribute

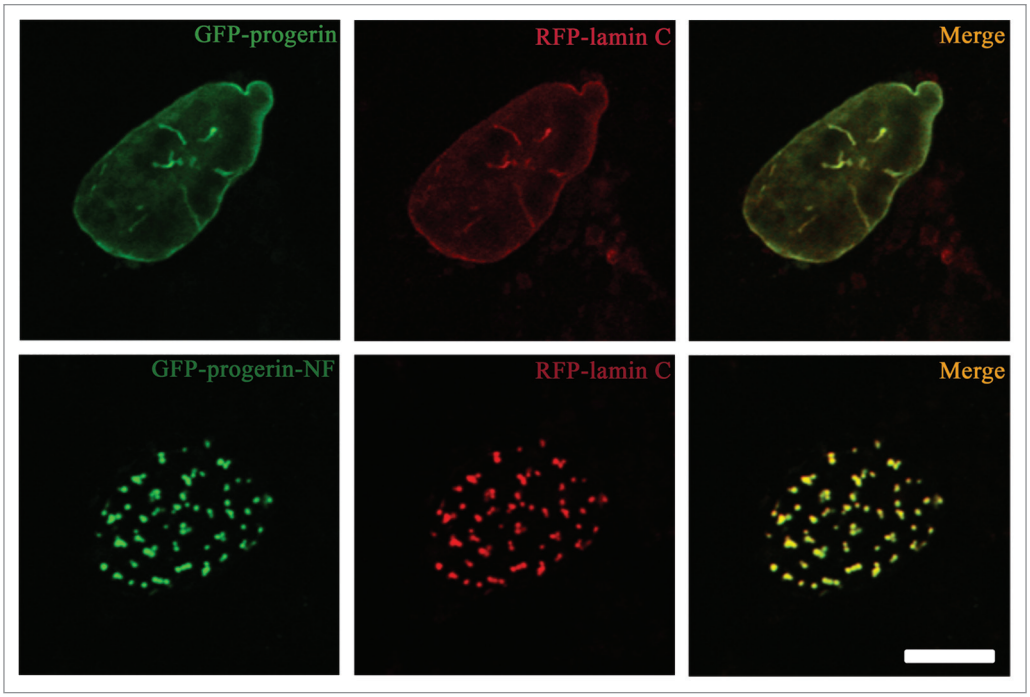

Figure 3. Expression of non-farnesylated progerin alters the nuclear distribution of lamin C in transiently transfected MEFs. Confocal fluorescence micrographs showing localizations of GFP-progerin and GFP-progerin-NF (green signals) with RFP-lamin C (red signals) in the same cells; merged images are shown at the right with signal overlap appearing yellow (merge). Bar: 5 μm.

discrete foci and other times in a more homogenous pattern.[17-21] Similar results have also been observed in cultured keratinocytes from transgenic mice expressing progerin.[27] In fibroblasts from two strains of knock in mice that expressed progerin with the CSIM sequence mutated to either SSIM or CSM, progerin was also primarily located away from the nuclear rim but localized to structures that looked like linear folds rather than punctate foci.[34,37] None of the previous studies on the effects of blocking farnesylation on progerin localization specifically analyzed its effects on the distribution of other A-type and B-type lamins. Our biochemical and biophysical results further suggest that non-farnesylated progerin associates more strongly with wild type lamin A and lamin C than farnesylated progerin.

We have confirmed these previous findings that non-farnesylated progerin concentrates in the nuclear interior. We have now shown that the diffusional mobility of non-farnesylated progerin is greater than that of its farnesylated counterpart at the nuclear periphery. We further showed that wild type A-type lamins preferentially associate with mis-localized non-farnesylated progerin in nuclei whereas the B-type lamin remains segregated from it. These results have potential implications for the therapeutic use of drugs that block protein prenylation to treat children with HGPS and also for basic mechanism of lamina formation.

FTIs and other drugs that block protein farnesylation are being studied in clinical trials of patients with HGPS.[42,43] However, the safety of long-term administration in such patients remains unknown. FTIs, alone or combined with a statin and aminobisphosphonate, have been shown to cause donut-shaped nuclei attributable to a centrosome separation defect in mitotic cells and blocking farnesylation of lamin B1 has been linked to this defect.[44] We have seen occasional post-mitotic fibroblasts from human subjects with HGPS showing donut-shaped nuclei after FTI treatment (data not shown) but did not see this in transfected cells expressing GFP-progerin or GFP-progerin-NF with or without FTI treatment. Our result, however, suggest that FTI treatment at certain concentrations or dosages with the purpose of blocking progerin farnesylation may elicit an unwanted cellular side effect, namely the redistribution of A-type lamins to the nuclear interior. Deficiency of A-type lamins from the lamina could lead to pathologies. Along these lines, *Lmna* null mice, which have no A-type lamins in the lamina, have severe skeletal and cardiac myopathies and peripheral neuropathy, dying at about 8 weeks of age.[45,46] Human subjects with mutations causing haploinsufficiency of A-type lamins also have severe myopathies and sometimes peripheral neuropathy.[47,48] Our finding that FTI treatment does not significantly affect the intranuclear localization of B-type lamins is consistent with previously observations.[49]

We also observed a partial co-localization of emerin with intranuclear foci of non-farnesylated progerin. Absence of emerin from the nuclear envelope occurs in most cases of X-linked Emery-Dreifuss muscular dystrophy.[50,51] While emerin is an integral membrane protein primarily localized at the nuclear envelope, the wild type protein is sometimes seen to a small extent in intranuclear foci, probably representing nuclear envelope invaginations.[52,53] Our present results in cells expressing GFP-progerin-NF are consistent with those showing that emerin also co-localizes with intranuclear foci of some lamin A variants that

©2012 Landes Bioscience. Do not distribute

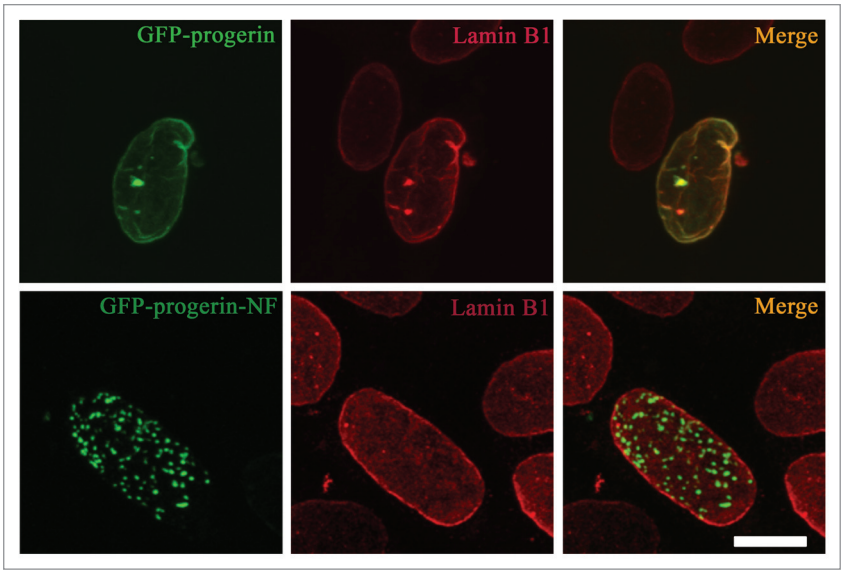

Figure 4. Expression of non-farnesylated progerin does not significantly alter the nuclear distribution of lamin B1 in transiently transfected MEFs. Confocal fluorescence micrographs showing localizations of GFP-progerin and GFP-progerin-NF (green signals) and immunofluorescence labeling with anti-lamin B1 antibodies (red signals) in the same cells; merged images are shown at the right with signal overlap appearing yellow (merge). Bar: 5 μm.

are associated with autosomal dominant Emery-Dreifuss muscular dystrophy.[54] These intranuclear foci are likely to be near the inner nuclear membrane, inducing micro-invaginations of inner nuclear membrane and allowing emerin, a transmembrane protein, to co-localize with them.[54] The localized binding to an A-type lamin likely prevents emerin from redistributing into the endoplasmic reticulum, as it does in cells lacking A-type lamins.[45] Given the observed effects of non-farnesylated progerin on A-type lamin and emerin redistribution, monitoring subjects with HGPS for adverse events involving striated muscle and nerve in clinical trials of protein farnesylation inhibitors would be prudent.

Our finding of a preferential association of lamin A and lamin C compared with lamin B1 with non-farnesylated progerin provide additional evidence for the existence of lamin microdomains as proposed by Goldman and collaborators.[55] In vitro, lamin A, lamin B1, lamin B2 and lamin C all can bind to each other, although with different affinities leading to differences in the stabilities of polymers composed of different lamins.[56,57] Within the cell nuclei expressing these four major lamins, however, A-type and B-type lamins form separate but interacting stable meshworks in the lamina.[55] FRET experiments in nuclei have similarly shown that lamins A and B1 polymerize in distinct homopolymers that further interact with homopolymers of the opposite type within the lamina and the nucleoplasm.[58] Farnesylated progerin can co-assemble in nuclei with lamin B1 and lamin A to form a mixed heteropolymer and lead to a loss of A-type and B-type lamin segregation at the nuclear lamina.[58] Our results suggest that non-farnesylated progerin preferentially binds to A-type lamins relative to lamin B1. Non-farnesylated progerin also may bind more strongly than farnesylated progerin to wild type A-type lamins. Hence, blocking farnesylation of progerin may lead to some degree of reestablishment of A-type and B-type lamin segregation into microdomains in HGPS.

We close by cautioning that all of our results were obtained in transfected cultured cells. Experiments to clearly differentiate intranuclear localization of non-farnesylated progerin from other A-type lamins at high resolution in animal tissues would be fraught with obvious technical hurdles. In perhaps the most relevant experiment in animal tissue, Yang et al. performed an analysis of non-farnesylated progerin localization in one animal tissue, the liver.[37] In liver sections of knock-in mice expressing non-farnesylated variants of progerin, they reported rarely observing abnormal shaped nuclei yet most of the non-farnesylated progerin was located at the nuclear rim. Liver is not significantly affected in HGPS.[1,2] In our own study of transgenic mice expressing progerin in keratinocytes, we did not observe significant intranuclear progerin in skin sections of mice treated with either a FTI or a statin plus an aminobisphosphonate leading to approximately 15% to 20% inhibition of protein prenylation, although abnormal nuclear morphology was improved.[30] These mice, despite having nuclear structural abnormalities in keratinocytes, had normal skin structure and function.[27] All of the observations in cultured cells may therefore not apply to all animal tissues. The effects of non-farnesylated progerin on A-type lamin redistribution may also not be as dramatic in cells in native tissues as they are in transfected MEFs overexpressing the protein. Nonetheless, our results clearly show that non-farnesylated progerin has the potential to affect A-type lamin distribution and possibly function.

Materials and Methods

Plasmid construction. We first generated a plasmid that contained a cDNA for full-length human prelamin A fused to GFP at its N-terminus by ligation of a previously described cDNA[59] into the *XhoI* and BamHI sites of pEGFP-C1 (Clontech). To construct an expression plasmid encoding GFP-progerin, a cDNA encoding progerin in pSVF[27] was digested with *BsiWI* and BamHI and the reaction product was ligated into the plasmid encoding GFP-lamin A from which the coding cDNA was removed by treatment with the same restriction endonucleases. To produce a cDNA encoding GFP fused to non-farnesylated progerin, progerin cDNA was used as a template for polymerase chain reaction with a 3' oligonucleotide primer of sequence 5'-ATG GAT CCT TAC ATG ATG CTG CTG TTC TG-3'. This reaction generated a cDNA encoding a cysteine to serine substitution at amino acid 611 of progerin, changing the carboxyl-terminal CSIM to SSIM. This cDNA was digested with *BsiWI* and BamHI and ligated into the plasmid encoding GFP-lamin A from which the cDNA was removed by digestion with the same restriction endonuclease.

©2012 Landes Bioscience. Do not distribute

To generate a construct encoding RFP fused to the N-terminus of lamin C, mouse lamin C cDNA was generated from reverse transcribed mRNA isolated from MEFs. Restriction sites BglII (5') and *XbaI* (3') were engineered into the cDNA by polymerase chain reaction using primers 5'-ACT AGA TCT GTC ACC CTG CCG GCC ATG-3' and 5'-TAT CTA GAT CAG CGG CGG CTG CCA CTC A-3', respectively. The reaction product was subcloned into the pEGFP-C1 in which the EGFP coding region was replaced by monomeric RFP coding region.[60] The plasmid encoding RFP-lamin A has been described previously.[60] Sequencing of cDNA constructs was performed at the Herbert Irving Comprehensive Cancer Center DNA Sequencing Lab at Columbia University Medical Center.

Cell culture, transfection and FTI treatment. Immortalized MEFs were cultured in Dulbecco's modified Eagle medium containing 10% fetal bovine serum at 37°C and 5% CO_2. Cells were transiently transfected using Lipofectamine PLUS following the manufacturer's instructions (Life Technologies). FTI-276 (Sigma) at a final concentration of 10 μM from a stock solution in dimethyl sulfoxide, or an equal volume of dimethyl sulfoxide as a control, was added to culture media 4 h after starting transfection for a total of 48 h.

Fluorescence microscopy. Fluorescence microscopy to detect GFP or RFP fluorescence or fluorescence after immunostaining was performed as described previously.[59,60] When imaging cells for GFP or RFP fluorescence, we selected those with moderate protein expression levels defined a clear nuclear rim fluorescence visible under the microscope and on the screen of the Zeiss LSM Image Browser window with detective gain set at 400–500 and a pinhole size of 256. For immunofluorescence microscopy, cells cultured on chamber slides were immunostained as described previously.[59,60] Primary antibodies used were rabbit polyclonal anti-lamin A (sc-20680, Santa Cruz) at a dilution of 1:2,000 dilution, rabbit polyclonal anti-lamin B1[61] at a dilution of 1:1,000, rabbit polyclonal anti-LAP1[62] at a dilution of 1:500, mouse monoclonal anti-emerin (Vector Laboratories) at a dilution of 1:30, mouse monoclonal Mab414 anti-nuclear pore complex (Abcam) at a dilution of 1:4,000, rabbit polyclonal anti-HP1[63] at a dilution of 1:150, mouse monoclonal anti-RNAPII CTD repeat YSPTSPS (Abcam) at a dilution of 1:1,000, rabbit polyclonal anti-PML (Abcam) at a dilution of 1:200 and rabbit polyclonal anti-PCNA (Abcam) at a dilution of 1:200. Secondary antibodies were Rhodamine Red-X-conjugated goat anti-rabbit IgG (Jackson ImmunoResearch Laboratories) and Texas Red goat anti-mouse IgG (Life Technologies) at a dilution of 1:200. Microscopy was performed on a Zeiss LSM 510 META confocal laser scanning system attached to a Zeiss Axiovert 200 inverted microscope with spectral resolution of fluorescence labels and excitations at 488 nm and 543 nm (Carl Zeiss). We generated z-series by scanning a stack consisting of 15–20 optical sections

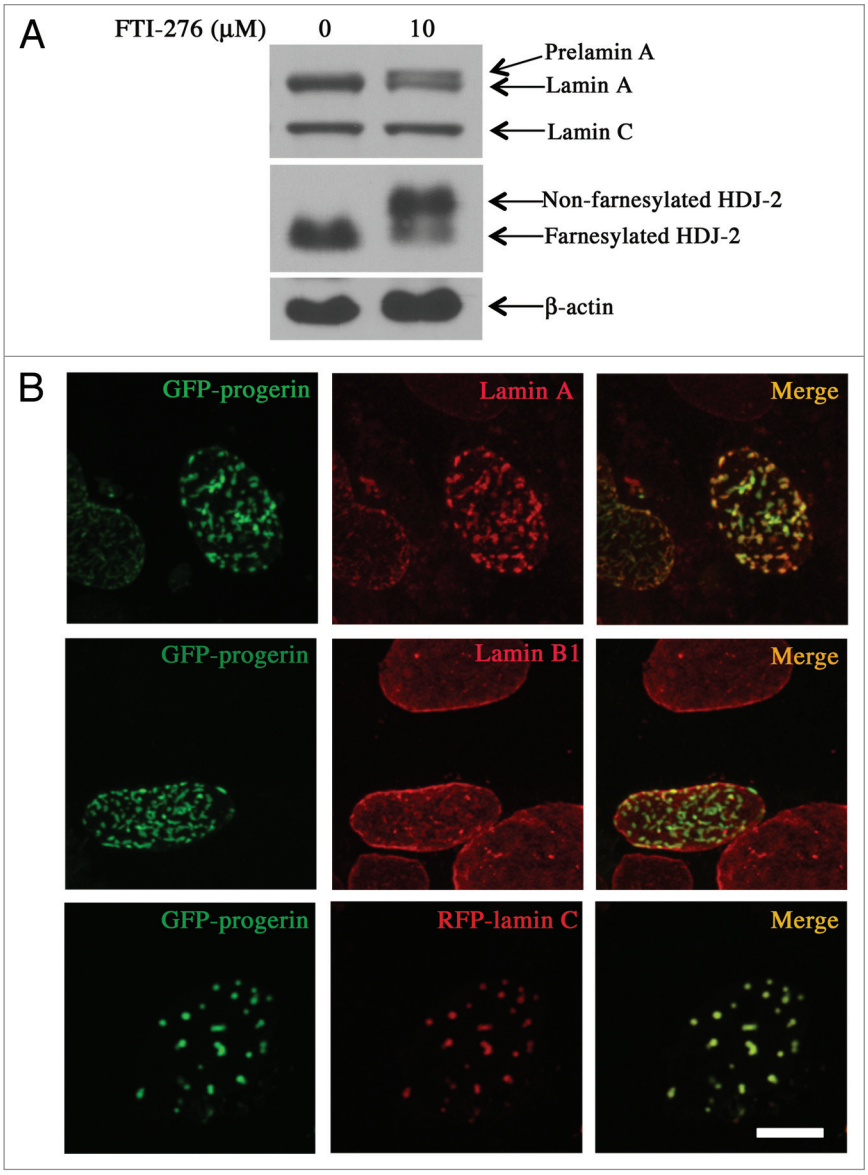

Figure 5. Effects of FTI treatment on protein farnesylation, progerin localization and intranuclear distribution of lamins. (A) FTI treatment blocks protein farnesylation in MEFs. MEFs were incubated for 48 h with 0 μM or 10 μM FTI-276 and extracted proteins were separated by SDS-PAGE and immunoblotted with antibodies against lamin A/C, HDJ-2 and β-actin. (B) Treatment of MEFs with FTI leads to intranuclear localization of GFP-progerin and altered distributions of lamin A and lamin C but not lamin B1. Confocal fluorescence micrographs showing localizations of GFP-progerin (green signals), immunofluorescence labeling with anti-lamin A antibodies (red signals, top row), immunofluorescence labeling with anti-lamin B1 antibodies (red signals, middle row) and RFP-lamin C (red signals, bottom row) in cells that were incubated with 10 μM FTI-276; merged images are shown at the right with signal overlap appearing yellow (merge). Bar: 5 μm.

©2012 Landes Bioscience. Do not distribute

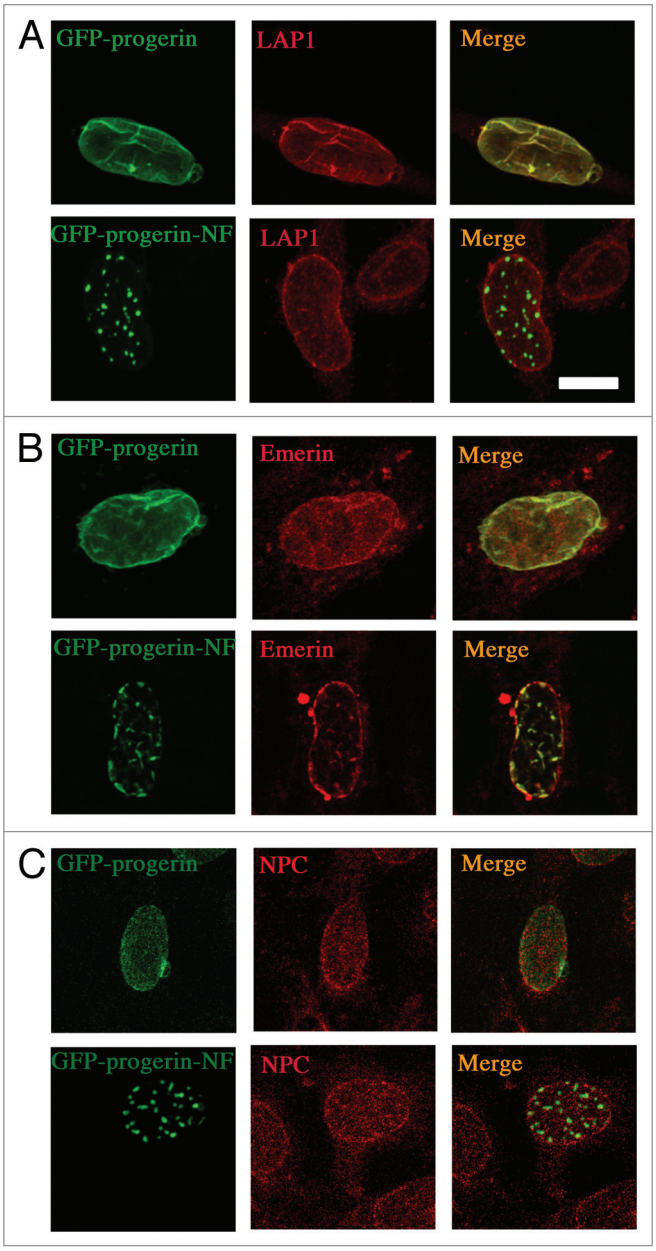

Figure 6. Effects of expressing non-farnesylated progerin on the distribution of two integral proteins of the inner nuclear membrane and non-membrane nuclear pore complex (NPC) proteins. (A) Confocal fluorescence micrographs showing localizations of GFP-progerin and GFP-progerin-NF (green signals) and immunofluorescence labeling with anti-LAP1 antibodies (red signal). (B) Confocal fluorescence micrographs showing localizations of GFP-progerin and GFP-progerin-NF (green signals) and immunofluorescence labeling with anti-emerin antibodies (red signals). (C) Confocal fluorescence micrographs showing localizations of GFP-progerin and GFP-progerin-NF (green signals) and immunofluorescence labeling with antibodies that recognize NPC proteins (red signals). Merged images of the same cells are shown at the right of each panel with signal overlap appearing yellow (merge). Bar: 5 μm.

using a step size of 0.36 μm in the z-axis. Stacks of images were used to make Audio Video Interleave (AVI) files of 3-dimensional representations of nuclei using projections from the Zeiss LSM Image Browser.

FRAP. MEFs were cultured on chambered cover glasses and transfected as described above for analysis by FRAP. Experiments were performed on the microscope described above using the 488 nm line with a 30mW argon laser in conjunction with a Plan-Neofluar 40×/1.3 oil objective (Carl Zeiss). A selected area with fixed size for each nucleus was photobleached at full laser power (100% transmission) for 25 iterations and the fluorescence recovery was monitored by scanning at low power (2.1% transmission) in 3 sec intervals for the first 30 micrographs and 8 sec intervals for another 70 micrographs. The average intensity of the fluorescence signal was measured in the region of interest using NIH Image J software (http://rsb.info.nih.gov/ij) and normalized to the change in total fluorescence as $I_{rel} = T_0 I_t / T I_0$ as described previously.[60] The mean normalized fluorescence plus or minus standard deviations calculated from 10 to 12 cells expressing the same fusion protein were plotted against time after bleach using Microsoft Excel. The significance of the difference in normalized fluorescence between cells expressing the different fusion proteins was determined using student's t-tests at multiple time points (13 sec, 22 sec, 31 sec, 61 sec, 102 sec, 302 sec and 654 sec).

Protein isolation, electrophoresis and immunoblotting. Immunoblotting was performed to assess the effects of FTI treatment on protein farnesylation in cultured cells. Proteins were extracted from MEFs in urea isolation buffer, separated in SDS-polyacrylamide gels, transferred on nitrocellulose membranes and analyzed by immunoblotting as described elsewhere.[64] Primary antibodies used for immunoblotting were mouse anti-β-actin (Santa Cruz) at 1:5,000 dilution, mouse anti-HDJ-2 (Lab Vision) at 1:500 dilution and rabbit anti-lamin A/C (Santa Cruz) at 1:5,000 dilution. Secondary antibodies were ECL-horseradish peroxidase-conjugated anti-mouse and anti-rabbit antibodies (GE Healthcare) used at a dilution of 1:5,000. Signals were detected using SuperSignal West Pico Chemiluminescent Substrate Kit (Pierce) and X-ray film (Phenix Research Products).

Co-immunoprecipitation. Protein extracts were isolated from transiently transfected MEFs expressing GFP-lamin A, GFP-progerin, GFP-progerin-NF or GFP, then were subjected to co-immunoprecipitation using mouse monoclonal anti-GFP antibody ab1218 (Abcam). Co-immunoprecipitations were performed in triplicate with anti-GFP antibody using the Co-immunoprecipitation Kit following the manufacture's instruction (Pierce). Precipitated products were separated by SDS-PAGE and analyzed by immunoblotting with anti-lamin A/C antibodies as described above.

FRET. MEFs grown in chamber slides were co-transfected with plasmids expressing GFP-progerin or GFP-progerin-NF (donors) and either RFP-lamin A, RFP-lamin C or RFP (acceptors). MEFs also were transfected with plasmids expressing RFP-lamin A or GFP-progerin individually to calculate correction factors. Cells were fixed in methanol at -20°C for 6 min, washed in phosphate-buffered saline and mounted with a mounting medium without

©2012 Landes Bioscience. Do not distribute

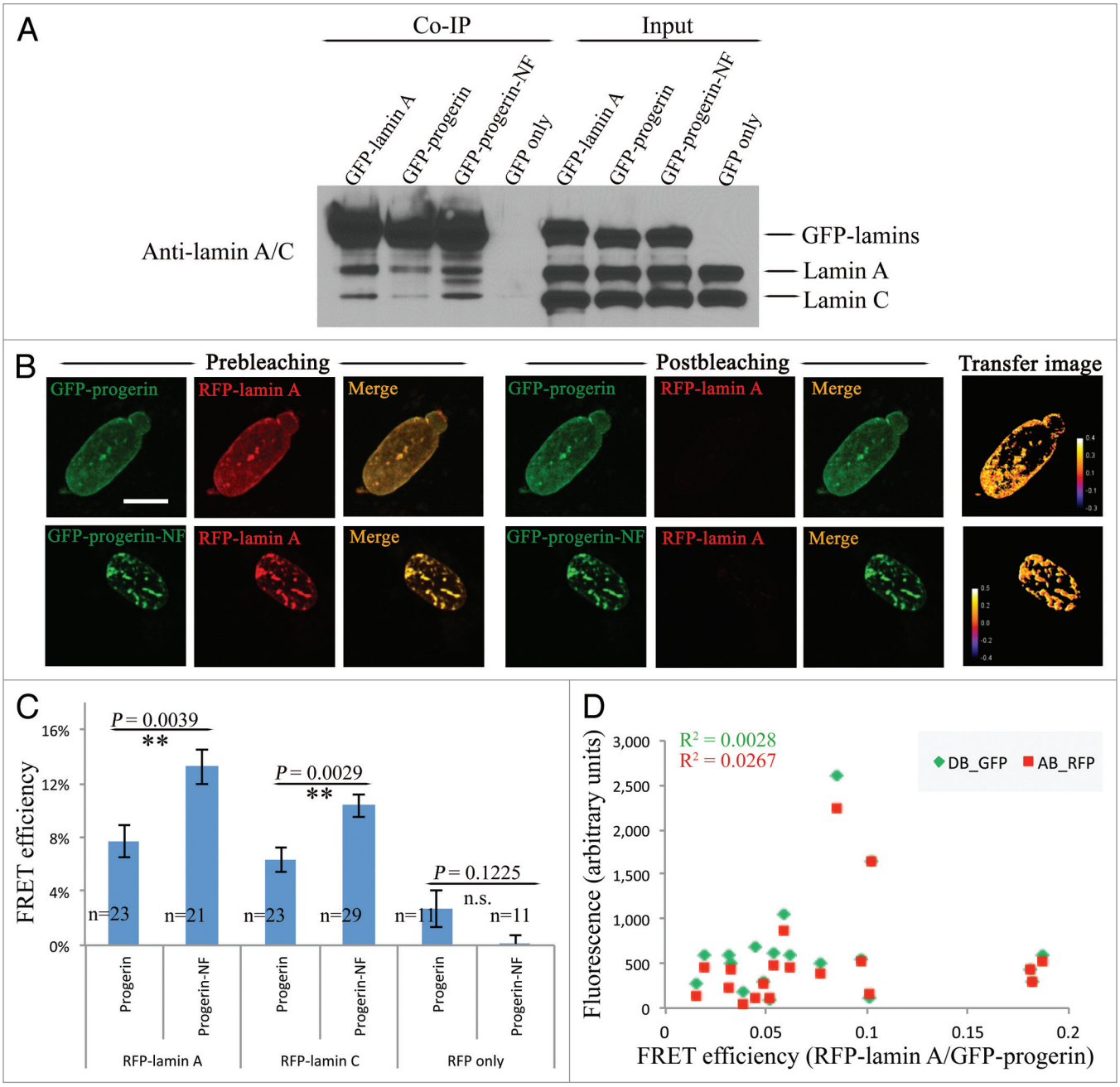

Figure 7. Binding of non-farnesylated progerin to A-type lamins. (A) Immunoblot with anti-lamin A/C antibodies of co-immunoprecipitated proteins (Co-IP) and inputs (Input) of cell extracts. MEFs transiently expressing GFP-lamin A, GFP-progerin, GFP-progerin-NF or GFP only were subjected to immunoprecipitation with antibody against GFP. Less endogenous lamin A and lamin C was precipitated from MEFs expressing GFP-progerin than GFP-lamin A or GFP-progerin-NF and no endogenous lamin A or lamin C was detected in precipitates from MEFs expressing only GFP. (B) Top row shows fluorescence micrographs of a cell expressing GFP-progerin (green) and RFP-lamin A (red) with merged image (yellow) and bottom row shows a cell expressing GFP-progerin-NF (green) and RFP-lamin A (red) with merged image (yellow). Images before photobleaching (Prebleaching), after photobleaching (Postbleaching) and energy transfer image (Transfer image) are indicated. Bar: 5μm. (C) Energy transfer efficiency between GFP progerin or GFP-progerin-NF and RFP-lamin A, RFP-lamin C or RFP only. Transfer efficiencies were significantly higher for GFP-progerin NF than for GFP-progerin (values shown are means plus or minus standard errors; p values calculated using Student's t-test, two-tailed, two-sample unequal variance). No significant difference (n.s.) was detected in energy transfer efficiency between RFP only and GFP-progerin or GFP-progerin-NF. (D) Correlation of energy transfer efficiency and corresponding RFP-lamin A (acceptor) or GFP-progerin (donor) fluorescence intensity before photobleaching. AB_RFP: acceptor before photobleaching (red squares); DB-GFP: donor before photobleaching (green diamonds). No correlation was observed between FRET efficiencies and GFP-progerin or RFP-lamin A fluorescence intensity before photobleaching; similar lack of correlation was seen between FRET efficiencies and GFP-progerin-NF or RFP-lamin C fluorescence intensity before photobleaching (not shown).

©2012 Landes Bioscience. Do not distribute

anti-fading agent. Cells displaying moderate levels of GFP and RFP fluorescence were selected for FRET analysis. The RFP signal in the whole nucleus was photobleached in 6 sec using a 561 nm diode laser at 100% laser output using NIS element AR software on a Nikon A1R MP inverted laser scanning confocal microscope. Images in both channels (488 nm and 561 nm) were captured before and after acceptor photobleaching. The donor channel was corrected for crosstalk and unintentional bleaching using images of single-transfected cells. Data analysis and calculation of energy transfer efficiency were performed as reported previously[60] using the ImageJ software with the AccPbFRET plugin.[65]

Disclosure of Potential Conflicts of Interest

No potential conflicts of interest were disclosed.

Acknowledgments

Supported by NIH/NICHD grant 1R01HD070713. We thank Dr William T. Dauer (University of Michigan) for the anti-LAP1 antibodies.

Supplemental Materials

Supplemental materials may be found here:
www.landesbioscience.com/journals/nucleus/article/21675/

References

1. DeBusk FL. The Hutchinson-Gilford progeria syndrome. Report of 4 cases and review of the literature. J Pediatr 1972; 80:697-724; PMID:4552697; http://dx.doi.org/10.1016/S0022-3476(72)80229-4.
2. Merideth MA, Gordon LB, Clauss S, Sachdev V, Smith AC, Perry MB, et al. Phenotype and course of Hutchinson-Gilford progeria syndrome. N Engl J Med 2008; 358:592-604; PMID:18256394; http://dx.doi.org/10.1056/NEJMoa0706898.
3. Eriksson M, Brown WT, Gordon LB, Glynn MW, Singer J, Scott L, et al. Recurrent de novo point mutations in lamin A cause Hutchinson-Gilford progeria syndrome. Nature 2003; 423:293-8; PMID:12714972; http://dx.doi.org/10.1038/nature01629.
4. De Sandre-Giovannoli A, Bernard R, Cau P, Navarro C, Amiel J, Boccaccio I, et al. Lamin a truncation in Hutchinson-Gilford progeria. Science 2003; 300:2055; PMID:12702809; http://dx.doi.org/10.1126/science.1084125.
5. McKeon FD, Kirschner MW, Caput D. Homologies in both primary and secondary structure between nuclear envelope and intermediate filament proteins. Nature 1986; 319:463-8; PMID:3453101; http://dx.doi.org/10.1038/319463a0.
6. Aebi U, Cohn J, Buhle L, Gerace L. The nuclear lamina is a meshwork of intermediate-type filaments. Nature 1986; 323:560-4; PMID:3762708; http://dx.doi.org/10.1038/323560a0.
7. Goldman AE, Maul G, Steinert PM, Yang HY, Goldman RD. Keratin-like proteins that coisolate with intermediate filaments of BHK-21 cells are nuclear lamins. Proc Natl Acad Sci U S A 1986; 83:3839-43; PMID:2424013; http://dx.doi.org/10.1073/pnas.83.11.3839.
8. Fisher DZ, Chaudhary N, Blobel G. cDNA sequencing of nuclear lamins A and C reveals primary and secondary structural homology to intermediate filament proteins. Proc Natl Acad Sci U S A 1986; 83:6450-4; PMID:3462705; http://dx.doi.org/10.1073/pnas.83.17.6450.
9. Lin F, Worman HJ. Structural organization of the human gene encoding nuclear lamin A and nuclear lamin C. J Biol Chem 1993; 268:16321-6; PMID:8344919.
10. Sinensky M, Fantle K, Trujillo M, McLain T, Kupfer A, Dalton MJ. The processing pathway of prelamin A. J Cell Sci 1994; 107:61-7; PMID:8175923.
11. Davies BS, Fong LG, Yang SH, Coffinier C, Young SG. The posttranslational processing of prelamin A and disease. Annu Rev Genomics Hum Genet 2009; 10:153-74; PMID:19453251; http://dx.doi.org/10.1146/annurev-genom-082908-150150.
12. Corrigan DP, Kuszczak D, Rusinol AE, Thewke DP, Hrycyna CA, Michaelis S, et al. Prelamin A endoproteolytic processing in vitro by recombinant Zmpste24. Biochem J 2005; 387:129-38; PMID:15479156; http://dx.doi.org/10.1042/BJ20041359.
13. Davies BS, Coffinier C, Yang SH, Barnes RH 2nd, Jung HJ, Young SG, et al. Investigating the purpose of prelamin A processing. Nucleus 2011; 2:4-9; PMID:21647293; http://dx.doi.org/10.4161/nucl.2.1.13723.
14. Goldman RD, Shumaker DK, Erdos MR, Eriksson M, Goldman AE, Gordon LB, et al. Accumulation of mutant lamin A causes progressive changes in nuclear architecture in Hutchinson-Gilford progeria syndrome. Proc Natl Acad Sci U S A 2004; 101:8963-8; PMID:15184648; http://dx.doi.org/10.1073/pnas.0402943101.
15. Bridger JM, Kill IR. Aging of Hutchinson-Gilford progeria syndrome fibroblasts is characterised by hyperproliferation and increased apoptosis. Exp Gerontol 2004; 39:717-24; PMID:15130666; http://dx.doi.org/10.1016/j.exger.2004.02.002.
16. Yang SH, Bergo MO, Toth JI, Qiao X, Hu Y, Sandoval S, et al. Blocking protein farnesyltransferase improves nuclear blebbing in mouse fibroblasts with a targeted Hutchinson-Gilford progeria syndrome mutation. Proc Natl Acad Sci U S A 2005; 102:10291-6; PMID:16014412; http://dx.doi.org/10.1073/pnas.0504641102.
17. Toth JI, Yang SH, Qiao X, Beigneux AP, Gelb MH, Moulson CL, et al. Blocking protein farnesyltransferase improves nuclear shape in fibroblasts from humans with progeroid syndromes. Proc Natl Acad Sci U S A 2005; 102:12873-8; PMID:16129834; http://dx.doi.org/10.1073/pnas.0505767102.
18. Capell BC, Erdos MR, Madigan JP, Fiordalisi JJ, Varga R, Conneely KN, et al. Inhibiting farnesylation of progerin prevents the characteristic nuclear blebbing of Hutchinson-Gilford progeria syndrome. Proc Natl Acad Sci U S A 2005; 102:12879-84; PMID:16129833; http://dx.doi.org/10.1073/pnas.0506001102.
19. Mallampalli MP, Huyer G, Bendale P, Gelb MH, Michaelis S. Inhibiting farnesylation reverses the nuclear morphology defect in a HeLa cell model for Hutchinson-Gilford progeria syndrome. Proc Natl Acad Sci U S A 2005; 102:14416-21; PMID:16186497; http://dx.doi.org/10.1073/pnas.0503712102.
20. Glynn MW, Glover TW. Incomplete processing of mutant lamin A in Hutchinson-Gilford progeria leads to nuclear abnormalities, which are reversed by farnesyltransferase inhibition. Hum Mol Genet 2005; 14:2959-69; PMID:16126733; http://dx.doi.org/10.1093/hmg/ddi326.
21. McClintock D, Gordon LB, Djabali K. Hutchinson-Gilford progeria mutant lamin A primarily targets human vascular cells as detected by an anti-Lamin A G608G antibody. Proc Natl Acad Sci U S A 2006; 103:2154-9; PMID:16461887; http://dx.doi.org/10.1073/pnas.0511133103.
22. Scaffidi P, Misteli T. Reversal of the cellular phenotype in the premature aging disease Hutchinson-Gilford progeria syndrome. Nat Med 2005; 11:440-5; PMID:15750600; http://dx.doi.org/10.1038/nm1204.
23. Paradisi M, McClintock D, Boguslavsky RL, Pedicelli C, Worman HJ, Djabali K. Dermal fibroblasts in Hutchinson-Gilford progeria syndrome with the lamin A G608G mutation have dysmorphic nuclei and are hypersensitive to heat stress. BMC Cell Biol 2005; 6:27; PMID:15982412; http://dx.doi.org/10.1186/1471-2121-6-27.
24. Huang S, Chen L, Libina N, Janes J, Martin GM, Campisi J, et al. Correction of cellular phenotypes of Hutchinson-Gilford Progeria cells by RNA interference. Hum Genet 2005; 118:444-50; PMID:16208517; http://dx.doi.org/10.1007/s00439-005-0051-7.
25. Liu Y, Rusiñol A, Sinensky M, Wang Y, Zou Y. DNA damage responses in progeroid syndromes arise from defective maturation of prelamin A. J Cell Sci 2006; 119:4644-9; PMID:17062639; http://dx.doi.org/10.1242/jcs.03263.
26. Verstraeten VL, Ji JY, Cummings KS, Lee RT, Lammerding J. Increased mechanosensitivity and nuclear stiffness in Hutchinson-Gilford progeria cells: effects of farnesyltransferase inhibitors. Aging Cell 2008; 7:383-93; PMID:18331619; http://dx.doi.org/10.1111/j.1474-9726.2008.00382.x.
27. Wang Y, Panteleyev AA, Owens DM, Djabali K, Stewart CL, Worman HJ. Epidermal expression of the truncated prelamin A causing Hutchinson-Gilford progeria syndrome: effects on keratinocytes, hair and skin. Hum Mol Genet 2008; 17:2357-69; PMID:18442998; http://dx.doi.org/10.1093/hmg/ddn136.
28. Fong LG, Vickers TA, Farber EA, Choi C, Yun UJ, Hu Y, et al. Activating the synthesis of progerin, the mutant prelamin A in Hutchinson-Gilford progeria syndrome, with antisense oligonucleotides. Hum Mol Genet 2009; 18:2462-71; PMID:19376814; http://dx.doi.org/10.1093/hmg/ddp184.
29. Yang SH, Qiao X, Farber E, Chang SY, Fong LG, Young SG. Eliminating the synthesis of mature lamin A reduces disease phenotypes in mice carrying a Hutchinson-Gilford progeria syndrome allele. J Biol Chem 2008; 283:7094-9; PMID:18178963; http://dx.doi.org/10.1074/jbc.M708138200.
30. Wang Y, Östlund C, Worman HJ. Blocking protein farnesylation improves nuclear shape abnormalities in keratinocytes of mice expressing the prelamin A variant in Hutchinson-Gilford progeria syndrome. Nucleus 2010; 1:432-9; PMID:21326826.
31. Cao K, Graziotto JJ, Blair CD, Mazzulli JR, Erdos MR, Krainc D, et al. Rapamycin reverses cellular phenotypes and enhances mutant protein clearance in Hutchinson-Gilford progeria syndrome cells. Sci Transl Med 2011; 3:89ra58; PMID:21715679; http://dx.doi.org/10.1126/scitranslmed.3002346.
32. Yang SH, Meta M, Qiao X, Frost D, Bauch J, Coffinier C, et al. A farnesyltransferase inhibitor improves disease phenotypes in mice with a Hutchinson-Gilford progeria syndrome mutation. J Clin Invest 2006; 116:2115-21; PMID:16862216; http://dx.doi.org/10.1172/JCI28968.

©2012 Landes Bioscience. Do not distribute

33. Yang SH, Qiao X, Fong LG, Young SG. Treatment with a farnesyltransferase inhibitor improves survival in mice with a Hutchinson-Gilford progeria syndrome mutation. Biochim Biophys Acta 2008; 1781:36-9; PMID:18082640; http://dx.doi.org/10.1016/j.bbalip.2007.11.003.
34. Yang SH, Andres DA, Spielmann HP, Young SG, Fong LG. Progerin elicits disease phenotypes of progeria in mice whether or not it is farnesylated. J Clin Invest 2008; 118:3291-300; PMID:18769635; http://dx.doi.org/10.1172/JCI35876.
35. Capell BC, Olive M, Erdos MR, Cao K, Faddah DA, Tavarez UL, et al. A farnesyltransferase inhibitor prevents both the onset and late progression of cardiovascular disease in a progeria mouse model. Proc Natl Acad Sci U S A 2008; 105:15902-7; PMID:18838683; http://dx.doi.org/10.1073/pnas.0807840105.
36. Yang SH, Chang SY, Andres DA, Spielmann HP, Young SG, Fong LG. Assessing the efficacy of protein farnesyltransferase inhibitors in mouse models of progeria. J Lipid Res 2010; 51:400-5; PMID:19965595; http://dx.doi.org/10.1194/jlr.M002808.
37. Yang SH, Chang SY, Ren S, Wang Y, Andres DA, Spielmann HP, et al. Absence of progeria-like disease phenotypes in knock-in mice expressing a non-farnesylated version of progerin. Hum Mol Genet 2011; 20:436-44; PMID:21088111; http://dx.doi.org/10.1093/hmg/ddq490.
38. Young SG, Fong LG, Michaelis S. Prelamin A, Zmpste24, misshapen cell nuclei, and progeria--new evidence suggesting that protein farnesylation could be important for disease pathogenesis. J Lipid Res 2005; 46:2531-58; PMID:16207929; http://dx.doi.org/10.1194/jlr.R500011-JLR200.
39. Dahl KN, Scaffidi P, Islam MF, Yodh AG, Wilson KL, Misteli T. Distinct structural and mechanical properties of the nuclear lamina in Hutchinson-Gilford progeria syndrome. Proc Natl Acad Sci U S A 2006; 103:10271-6; PMID:16801550; http://dx.doi.org/10.1073/pnas.0601058103.
40. Holtz D, Tanaka RA, Hartwig J, McKeon F. The CaaX motif of lamin A functions in conjunction with the nuclear localization signal to target assembly to the nuclear envelope. Cell 1989; 59:969-77; PMID:2557160; http://dx.doi.org/10.1016/0092-8674(89)90753-8.
41. Lutz RJ, Trujillo MA, Denham KS, Wenger L, Sinensky M. Nucleoplasmic localization of prelamin A: implications for prenylation-dependent lamin A assembly into the nuclear lamina. Proc Natl Acad Sci U S A 1992; 89:3000-4; PMID:1557405; http://dx.doi.org/10.1073/pnas.89.7.3000.
42. Kieran MW, Gordon L, Kleinman M. New approaches to progeria. Pediatrics 2007; 120:834-41; PMID:17908771; http://dx.doi.org/10.1542/peds.2007-1356.
43. Pereira S, Bourgeois P, Navarro C, Esteves-Vieira V, Cau P, De Sandre-Giovannoli A, et al. HGPS and related premature aging disorders: from genomic identification to the first therapeutic approaches. Mech Ageing Dev 2008; 129:449-59; PMID:18513784; http://dx.doi.org/10.1016/j.mad.2008.04.003.
44. Verstraeten VL, Peckham LA, Olive M, Capell BC, Collins FS, Nabel EG, et al. Protein farnesylation inhibitors cause donut-shaped cell nuclei attributable to a centrosome separation defect. Proc Natl Acad Sci U S A 2011; 108:4997-5002; PMID:21383178; http://dx.doi.org/10.1073/pnas.1019532108.
45. Sullivan T, Escalante-Alcalde D, Bhatt H, Anver M, Bhat N, Nagashima K, et al. Loss of A-type lamin expression compromises nuclear envelope integrity leading to muscular dystrophy. J Cell Biol 1999; 147:913-20; PMID:10579712; http://dx.doi.org/10.1083/jcb.147.5.913.
46. De Sandre-Giovannoli A, Chaouch M, Kozlov S, Vallat JM, Tazir M, Kassouri N, et al. Homozygous defects in LMNA, encoding lamin A/C nuclear-envelope proteins, cause autosomal recessive axonal neuropathy in human (Charcot-Marie-Tooth disorder type 2) and mouse. Am J Hum Genet 2002; 70:726-36; PMID:11799477; http://dx.doi.org/10.1086/339274.
47. Bonne G, Di Barletta MR, Varnous S, Bécane HM, Hammouda EH, Merlini L, et al. Mutations in the gene encoding lamin A/C cause autosomal dominant Emery-Dreifuss muscular dystrophy. Nat Genet 1999; 21:285-8; PMID:10080180; http://dx.doi.org/10.1038/6799.
48. Walter MC, Witt TN, Weigel BS, Reilich P, Richard P, Pongratz D, et al. Deletion of the LMNA initiator codon leading to a neurogenic variant of autosomal dominant Emery-Dreifuss muscular dystrophy. Neuromuscul Disord 2005; 15:40-4; PMID:15639119; http://dx.doi.org/10.1016/j.nmd.2004.09.007.
49. Dalton MB, Fantle KS, Bechtold HA, DeMaio L, Evans RM, Krystosek A, et al. The farnesyl protein transferase inhibitor BZA-5B blocks farnesylation of nuclear lamins and p21ras but does not affect their function or localization. Cancer Res 1995; 55:3295-304; PMID:7614464.
50. Nagano A, Koga R, Ogawa M, Kurano Y, Kawada J, Okada R, et al. Emerin deficiency at the nuclear membrane in patients with Emery-Dreifuss muscular dystrophy. Nat Genet 1996; 12:254-9; PMID:8589715; http://dx.doi.org/10.1038/ng0396-254.
51. Manilal S, Nguyen TM, Sewry CA, Morris GE. The Emery-Dreifuss muscular dystrophy protein, emerin, is a nuclear membrane protein. Hum Mol Genet 1996; 5:801-8; PMID:8776595; http://dx.doi.org/10.1093/hmg/5.6.801.
52. Östlund C, Ellenberg J, Hallberg E, Lippincott-Schwartz J, Worman HJ. Intracellular trafficking of emerin, the Emery-Dreifuss muscular dystrophy protein. J Cell Sci 1999; 112:1709-19; PMID:10318763.
53. Fairley EA, Kendrick-Jones J, Ellis JA. The Emery-Dreifuss muscular dystrophy phenotype arises from aberrant targeting and binding of emerin at the inner nuclear membrane. J Cell Sci 1999; 112:2571-82; PMID:10393813.
54. Holt I, Östlund C, Stewart CL, Man N, Worman HJ, Morris GE. Effect of pathogenic mis-sense mutations in lamin A on its interaction with emerin in vivo. J Cell Sci 2003; 116:3027-35; PMID:12783988; http://dx.doi.org/10.1242/jcs.00599.
55. Shimi T, Pfleghaar K, Kojima S, Pack CG, Solovei I, Goldman AE, et al. The A- and B-type nuclear lamin networks: microdomains involved in chromatin organization and transcription. Genes Dev 2008; 22:3409-21; PMID:19141474; http://dx.doi.org/10.1101/gad.1735208.
56. Ye Q, Worman HJ. Protein-protein interactions between human nuclear lamins expressed in yeast. Exp Cell Res 1995; 219:292-8; PMID:7628545; http://dx.doi.org/10.1006/excr.1995.1230.
57. Schirmer EC, Gerace L. The stability of the nuclear lamina polymer changes with the composition of lamin subtypes according to their individual binding strengths. J Biol Chem 2004; 279:42811-7; PMID:15284226; http://dx.doi.org/10.1074/jbc.M407705200.
58. Delbarre E, Tramier M, Coppey-Moisan M, Gaillard C, Courvalin JC, Buendia B. The truncated prelamin A in Hutchinson-Gilford progeria syndrome alters segregation of A-type and B-type lamin homopolymers. Hum Mol Genet 2006; 15:1113-22; PMID:16481358; http://dx.doi.org/10.1093/hmg/ddl026.
59. Ostlund C, Sullivan T, Stewart CL, Worman HJ. Dependence of diffusional mobility of integral inner nuclear membrane proteins on A-type lamins. Biochemistry 2006; 45:1374-82; PMID:16445279; http://dx.doi.org/10.1021/bi052156n.
60. Östlund C, Folker ES, Choi JC, Gomes ER, Gundersen GG, Worman HJ. Dynamics and molecular interactions of linker of nucleoskeleton and cytoskeleton (LINC) complex proteins. J Cell Sci 2009; 122:4099-108; PMID:19843581; http://dx.doi.org/10.1242/jcs.057075.
61. Cance WG, Chaudhary N, Worman HJ, Blobel G, Cordon-Cardo C. Expression of the nuclear lamins in normal and neoplastic human tissues. J Exp Clin Cancer Res 1992; 11:233-46.
62. Goodchild RE, Dauer WT. The AAA+ protein torsinA interacts with a conserved domain present in LAP1 and a novel ER protein. J Cell Biol 2005; 168:855-62; PMID:15767459; http://dx.doi.org/10.1083/jcb.200411026.
63. Sharma GG, Hwang KK, Pandita RK, Gupta A, Dhar S, Parenteau J, et al. Human heterochromatin protein 1 isoforms $HP1^{(Hsalpha)}$ and $HP1^{(Hsbeta)}$ interfere with hTERT-telomere interactions and correlate with changes in cell growth and response to ionizing radiation. Mol Cell Biol 2003; 23:8363-76; PMID:14585993; http://dx.doi.org/10.1128/MCB.23.22.8363-8376.2003.
64. Fong LG, Frost D, Meta M, Qiao X, Yang SH, Coffinier C, et al. A protein farnesyltransferase inhibitor ameliorates disease in a mouse model of progeria. Science 2006; 311:1621-3; PMID:16484451; http://dx.doi.org/10.1126/science.1124875.
65. Roszik J, Szöllosi J, Vereb G. AccPbFRET: an ImageJ plugin for semi-automatic, fully corrected analysis of acceptor photobleaching FRET images. BMC Bioinformatics 2008; 9:346; PMID:18713453; http://dx.doi.org/10.1186/1471-2105-9-346.

©2012 Landes Bioscience. Do not distribute